

Pressure-induced suppression of charge order and nanosecond valence dynamics in Fe_2OBO_3

G. R. Hearne,^{1,*} W. N. Sibanda,¹ E. Carleschi,¹ V. Pischedda,² and J. P. Attfield³

¹*Department of Physics, University of Johannesburg, P.O. Box 524, Auckland Park, 2006, Johannesburg, South Africa*

²*Laboratoire de Physique de la Matière Condensée et Nanostructures, University Lyon 1 and CNRS, 69622 Villeurbanne Cedex, France*

³*Centre for Science at Extreme Conditions and School of Chemistry, University of Edinburgh, Erskine Williamson Building, King's Buildings, Mayfield Road, Edinburgh EH9 3JZ, United Kingdom*

(Received 17 September 2012; published 26 November 2012)

Valence order and fluctuations in the mixed-valence warwickite Fe_2OBO_3 have been explored by ^{57}Fe Mössbauer effect spectroscopy at pressures up to 30 GPa in diamond anvil cell experiments. At room temperature a drastic disruption of charge order is evident at ~ 11 GPa. There is coexistence of charge order and a progressively increasing abundance of fluctuating valence states in the range extending to ~ 16 GPa. At $P > 16$ GPa only signatures of electron exchange relaxation, $\text{Fe}^{2+} \leftrightarrow \text{Fe}^{3+}$, where “ \leftrightarrow ” represents the resonating mobile carrier, are discerned. Spectral signatures indicate that electron hopping is on a timescale of ~ 50 ns, that is, in a time window to which the nuclear resonance technique is particularly sensitive. Low-temperature quenching (~ 110 K) at these high pressures (i) is not sufficient to inhibit electron exchange for charge order to reemerge and (ii) reveals that magnetic ordering typical of the charge-ordered phase at low pressure is completely altered to entail new spin dynamics. This evidences the strong interplay between charge order and magnetism and establishes $P \sim 16$ GPa as a new electronic phase transition boundary for this system. Nanosecond valence fluctuation signatures persist upon further pressurization to ~ 30 GPa at 300 K, suggestive of continued confinement of the mobile carrier to the $\text{Fe}^{2+} \leftrightarrow \text{Fe}^{3+}$ pair at these extremes.

DOI: [10.1103/PhysRevB.86.195134](https://doi.org/10.1103/PhysRevB.86.195134)

PACS number(s): 71.28.+d, 62.50.-p, 71.27.+a, 76.80.+y

Charge ordering (CO) refers to charge carriers localizing on ions, whereupon different integer valences are established to form an ordered pattern or superstructure within a crystal lattice. Many physical phenomena in transition-metal oxides, including colossal magnetoresistance and high-temperature superconductivity,^{1,2} appear to be related to CO, and there has been intense growing interest in this phenomenon in the last decade.³ More recently, the interplay between CO and *ferroelectricity*, in what is considered a new class of topical multiferroics, has generated much excitement in the condensed matter physics community.⁴⁻⁶

A long sought-after case of ionic CO has been claimed in the last several years. The low-temperature phase of iron oxoborate Fe_2OBO_3 is supposed to present the clearest example of ionic CO found so far;⁷ a nearly integer iron valence separation into Fe^{2+} and Fe^{3+} at $T \leq 280$ K has been demonstrated by ^{57}Fe Mössbauer effect (ME) spectroscopy, structural refinement, and electronic-structure calculations.^{7,8}

The warwickite crystal structure of Fe_2OBO_3 is depicted in Fig. 1, where ribbons formed by four Fe octahedral sites wide extend infinitely along the a axis. Note, from Fig. 1(b), there is triangular connectivity among sites on adjacent chains leading to geometrical (intraribbon) frustration for interactions between chains.^{8,9} Such triangular connectivity among chains on neighboring ribbons is also prevalent in the b - c plane perpendicular to the ribbon direction, leading to interribbon frustration effects.⁸ This results in energy degenerate configurations in both CO (domain formation)⁸ as well as in spin ordering (spin-cluster glass effects).^{10,11} The latter type of magnetic manifestations involving glassy dynamics have also been seen in geometrically frustrated LuFe_2O_4 , which exhibits CO as well.¹²

In Fe_2OBO_3 the electronic system is commensurately charge ordered at temperatures less than the onset $T_{\text{CCO}} \sim 280$ K, with its basic CO units being threaded pathways of

alternating Fe^{2+} and Fe^{3+} sites in the a axis direction;^{7,8} see Fig. 1. Total CO is established over microdomains because of the energy degeneracy of various valence separation configurations.^{8,13} Temperature-dependent lattice incommensurate CO has recently been found in the intermediate-temperature range, $280 \text{ K} < T < 340 \text{ K}$.^{8,14} This is also attributed to energy degenerate CO configurations from geometrical frustration effects and the consequent occurrence of thermally activated mobile antiphase boundaries.⁸ A valence-fluctuating state (melted CO, viz., $\text{Fe}^{2+} \leftrightarrow \text{Fe}^{3+}$ electron hopping) ensues at $T > 340$ K. There is a concomitant structural adjustment from monoclinic \rightarrow orthorhombic symmetry when this high-temperature valence-fluctuating phase is realized.⁸

The compound is weakly ferromagnetic (onset at $T_M = 155$ K) as a result of both the CO and “up”/“down” spin orientations on the structurally distinct Fe(1) and Fe(2) sites in each ribbon. The net magnetic moment is $< 0.1 \mu_B$ per formula unit from near cancellation of the antiparallel moments, depicted in Fig. 1(a).^{15,16}

It is natural to contemplate what the response of the CO state to pressurization would be. This is expected to “tune” the competition between strong *onsite* (Hubbard U) and *intersite* (V) Coulomb interactions, which have a governing role in the establishment of CO. This could lend further insight into the mechanism of CO and what is the effect of such unit cell volume changes on the magnetic-electronic properties. The high-temperature transition from the incommensurate to the disordered phase is thought to be related to the onsite Coulomb repulsion (Hubbard U) and the intersite V from intrachain Coulomb repulsion. The commensurate CO results from the contribution of interchain interactions.¹⁷ Pressure can thus be anticipated as a pertinent tuning parameter of these transitions and the geometrical frustration, so as to elucidate the driving mechanisms.

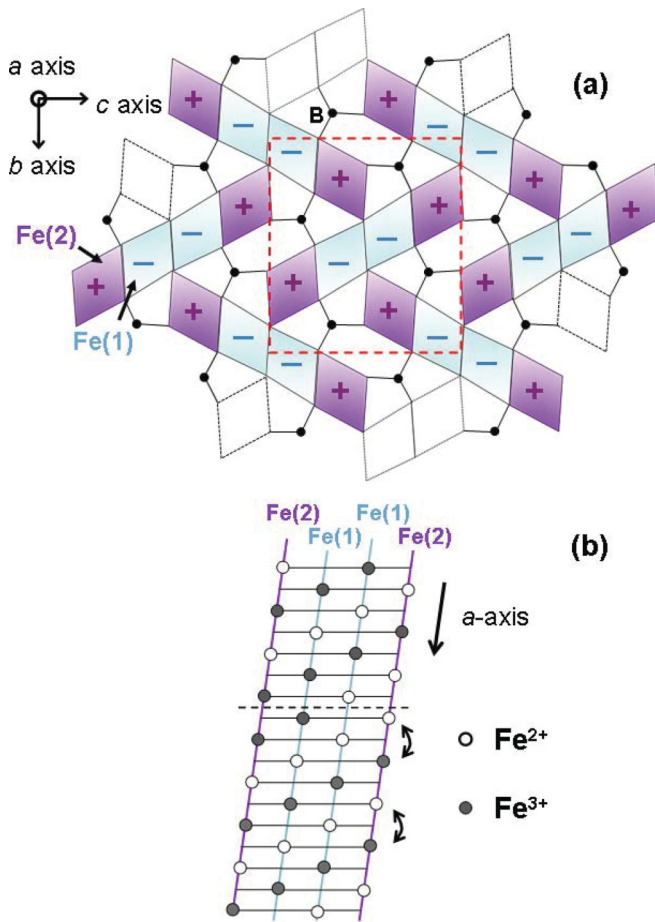


FIG. 1. (Color online) The warwickite crystal structure of Fe_2OBO_3 , adapted from Attfield *et al.*¹³ (a) In the b - c plane, this can be represented as Fe(2)-Fe(1)-Fe(1)-Fe(2) edge-sharing octahedra within a ribbon. There are structurally distinct iron octahedral sites, Fe(1) and Fe(2), that make up such four-chain ribbons. The “+” and “-” signs refer to antiparallel magnetic moments in the magnetically ordered phase. (b) The ribbon in the CO phase comprised of chains of four edge-sharing FeO_6 octahedra that extend infinitely along the crystallographic a axis. Dashed line indicates an antiphase boundary.

To the best of our knowledge, there has been only one pressure tuning experiment on this compound¹⁷ to ~ 2 GPa involving transport experiments on single-crystal specimens. Within this limited pressure regime, the incommensurate phase \rightarrow fluctuating-valence state transition (~ 340 K) is independent of pressure. The lower temperature commensurate to incommensurate phase transition point, T_{CCO} , increases at ~ 10 K/GPa. It may be inferred from this that at 4–6 GPa the temperature window for the incommensurate phase is closed, and only the commensurate CO \rightarrow fluctuating-valence phase transition can be anticipated in this pressure regime.

In this paper we *directly* probe the Fe electronic state and associated evolution of CO to much higher pressures by ^{57}Fe ME spectroscopy. Samples of natural isotopic abundance (2% ^{57}Fe) used in this work were from the batch of Attfield *et al.*^{13,15} in the original discovery of CO in this system. Both x-ray diffraction and ^{57}Fe ME spectroscopy at ambient pressure confirm that no sample degradation occurred. The powdered sample has been loaded into the 250- μm diameter cavity of a

Re gasket in a Merrill-Basset diamond anvil cell (DAC). Initial sample thickness was in the range 30–35 μm with Daphne oil also loaded as a pressure-transmitting medium. Pressures have been obtained from the R1-fluorescence of ruby ball markers loaded into the sample cavity. Quoted pressures are the average values from the 5–10% pressure distribution in the central two-thirds of the cavity. Details of the ME methodology may be found in Ref. 18.

Figure 2(a) shows the evolution of ME spectra up to 16 GPa. Distinct signatures of separate Fe^{3+} and Fe^{2+} valences are evident up to ~ 8 GPa, namely, respective resonance dips at ~ 0.3 mm/s and ~ 2 mm/s of the x scale (Doppler velocity) axis. The Lorentzian subcomponents have been depicted, where widely split doublets represent Fe^{2+} sites of differently distorted Fe(1) and Fe(2) octahedra in a ribbon (four chains wide in the b - c plane, Fig. 1). The centralized broadened doublet at ~ 0.3 mm/s models the two structurally distinct Fe^{3+} sites, $\text{Fe}^{3+}(2)$ and $\text{Fe}^{3+}(1)$, as well as some contribution from regions of the sample where electron exchange is occurring near domain boundaries of the incommensurate CO phase.⁸ Hence, a combination of three components has been condensed into the centralized doublet.^{16,19,20}

Drastic modifications to the spectral envelope are manifest at 11 GPa, where a new spectral component has emerged. This component’s onset at lower pressures is masked by other (Fe^{3+}) overlapping components. Such changes are conspicuous in the spectrum at 14.5 GPa, where there is also a concomitant drastic reduction in the intensities of Fe^{2+} components at ~ 2 mm/s. This spectrum appears to be dominated by a doublet with asymmetric relative intensities. It has been modeled as such, and fitting an asymmetric doublet permits extraction of reliable fitting parameters of the doublet splitting and its centroid. Figure 2(b) depicts the behavior of one of the spectral parameters of each of the subcomponents, namely, the isomer shift (IS; centroid), used to identify Fe valences unambiguously.²⁰ This new high-pressure phase component has hyperfine interaction parameters of a quadrupole (doublet) splitting of QS ~ 0.7 mm/s and IS ~ 0.7 mm/s (IS values are quoted relative to α -Fe metal standard at 300 K). These values are intermediate between those of known Fe^{2+} and Fe^{3+} valences.^{7,20} Therefore, at ~ 16 GPa and beyond, we have the valence-fluctuating state exclusively at room temperature. The manifestation of this as a broadened doublet component with asymmetric relative intensities is rationalized later in the text.

Figure 2(c) is a plot of the relative abundances (obtained from the absorption areas) of subcomponents of the fitted spectra in Fig. 2(a). Fluctuating valence contributions in the low-pressure regime are obtained from the centralized doublet, after subtracting out the contribution of static Fe^{3+} sites. These Fe^{3+} sites are equal, on crystal chemistry grounds, to the abundance of Fe^{2+} static electron sites derived from the absorption areas of the widely split doublets. Sites at which there are valence fluctuations are supposed to occur at the CO domain/antiphase boundaries^{8,14} and represent $\sim 20\%$ of Fe sites in the structure at ambient pressure (incommensurate phase at 300 K). The decreasing trend in the pressure dependence of these sites is consistent with the earlier studies limited to 2 GPa,¹⁷ where it has been inferred that the temperature window in which the incommensurate phase occurs is closed

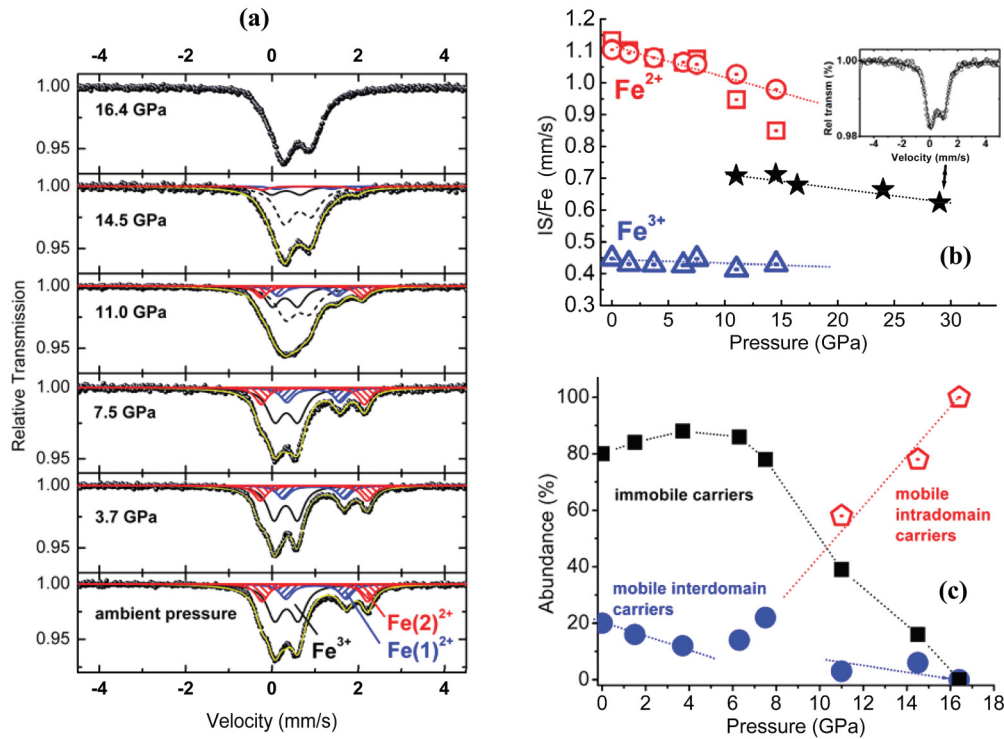


FIG. 2. (Color online) (a) Pressure evolution of ⁵⁷Fe ME spectra to ~16 GPa at room temperature. Solid line through the data points is the overall fit. Widely split doublets at low pressure represent Fe²⁺ in Fe(1) and Fe(2) octahedral sites (see text). The broadened central doublet represents the superposition of two corresponding Fe³⁺ valences at these sites, including a component (~20% abundance) representing thermally activated hopping at antiphase CO domain boundaries. Dashed line subcomponent at $P \geq 11$ GPa is the new high-pressure electronic phase from hopping proliferating within the original CO domains. (b) IS (centroid relative to α -Fe standard) indicative of Fe valence, at room temperature, of the various spectral subcomponents. Square (\blacksquare) and circle (\bullet) refer to ferrous Fe²⁺ (1) and Fe²⁺ (2) sites, respectively. Triangular (Δ) open symbol represents ferric Fe³⁺ sites. Transition to an intermediate valence state (\star) is conspicuously depicted here. The spectrum recorded at 30 GPa is in the inset; note asymmetric relative intensities of the doublet. Dotted lines are to guide the eye. (c) Pressure dependence of relative abundances of the subcomponents of spectra at room temperature. Assignment of these is to sites where there are (immobile) carriers localized in t_{2g} orbitals at Fe²⁺ sites and sites at which carriers are mobile from Fe²⁺ \leftrightarrow Fe³⁺ electron hopping. Dotted lines are to guide the eye.

by 4–6 GPa and CO is better stabilized. As P rises above ~6 GPa, valence fluctuations start to proliferate throughout the bulk of the domains, presumably where changes in interatomic distances (which may be intra- or interchain) within a ribbon have become significant. The associated spectral component, Fe^{2.5+}, emerges at this pressure, initially overlapping with and masked by the fitted centralized doublet.

The broadened doublet profile in the high-pressure regime $P > 16$ GPa, with asymmetric relative intensities and intermediate valence parameter values, is indicative of electron exchange relaxation. This profile, in analogy to various other temperature-dependent studies of dynamical charge transfer, is indicative of electron hopping on a timescale of ~50 ns.^{21,22} In a temperature-dependent study,⁷ such electron exchange (hopping) is concluded to occur along the a axis directed chains. Presumably, the pressure-instigated process occurs in the same way, as a result of interatomic spacing (primarily in the a axis direction) being reduced to below a critical value, whereupon the valence fluctuation process Fe²⁺ \leftrightarrow Fe³⁺ in the domains is triggered.

The ME spectrum of this high-pressure phase is relatively broad compared to the subcomponents fitted at low pressure,

perhaps indicative of two overlapping components with similar profiles. This may be illustrative of similar relaxation times and hopping frequencies (of ~20 MHz), associated with the two original distinctive pathways involving Fe(2) sites only and Fe(1) sites only; see Fig. 1.⁸ We have fitted this with a single broadened component to extract pertinent parameters, e.g., the IS value because of limitations mentioned in Ref. 19. The spectral profile of the high-pressure phase seems to be quite different from that of the high-temperature profile at ambient pressure, where two distinct spectral components can be readily discerned.^{8,16} The subcomponents in that case have been attributed to fast electron exchange (> 100 MHz) along different adjacent pathways directed along the a axis.⁸

We have also investigated the magnetism of this high-pressure phase by way of ME experiments at selected low temperatures. This has been effected in a top-loading liquid nitrogen cryostat system with the source and the DAC kept at the same temperature.¹⁸ A ME spectrum recorded at 163 K does not show evidence of cooperative spin ordering; see inset of Fig. 3 (i.e., no indication of magnetic hyperfine structure in the wings of the spectrum).¹⁶ The T_M of the low-pressure phase has not risen, at high pressure, to appreciably beyond its ambient

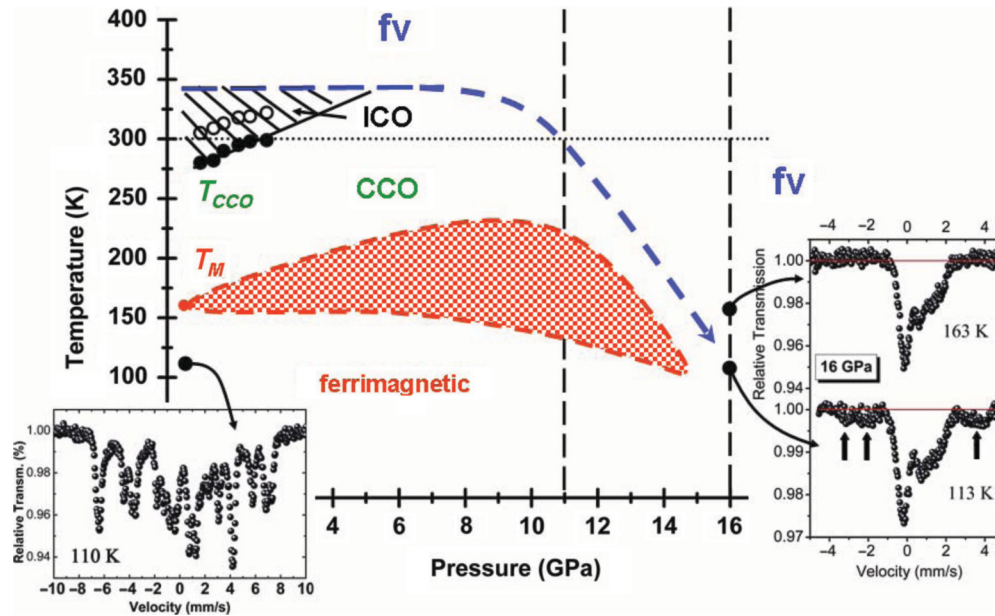


FIG. 3. (Color online) Qualitative (T, P) phase diagram based on pressure studies to date. Shaded area is the incommensurate CO (ICO) phase space from the studies of Akrap *et al.*¹⁷ Legends (CCO) and (fv) refer to commensurate charge-ordered and fluctuating valence states, respectively. At $P < 16$ GPa, both magnetic ordering temperatures T_M and phase boundary to the melted CO (fv) state at higher temperatures have not been investigated in detail and are rather depicted as evolving in the red checkerboard region and blue dashed line, respectively. Insets show ^{57}Fe ME spectra collected at low temperatures both at ambient pressure and 16 GPa (note different x axis velocity scales). Features at 16 GPa highlighted by arrows in the wings of the spectrum at 113 K are suggestive of PHS and associated spin-relaxation (spin-flip) processes (see text).

pressure value $T_M \sim 155$ K, signifying (imminent) collapse of magnetism in the high-pressure phase. Furthermore, lowering the temperature to well below the room-temperature valence-fluctuating state at 16 GPa does not freeze in the original charge order (i.e., absence of Fe^{2+} signatures; see 16 GPa, inset of Fig. 3). A further spectrum measured at 113 K presents similar features, except that there are weak indicators of magnetic hyperfine structure (emphasized by arrows in the wings of the spectrum, 16 GPa, inset of Fig. 3). This is not necessarily a signature of cooperative spin alignment. The resonance structure in the wings of the spectrum as well as the central pronounced asymmetric (doublet) features are signatures of paramagnetic hyperfine structure (PHS), involving spin-spin or spin-lattice relaxation.^{23–26} The complexity and features of this spectrum suggests spin relaxation times ranging from 0.1 to 10 ns.²³ This range is a consequence of a distribution of interaction pathways in the complex lattice structure with multiple Fe sites. The magnetism of the high-pressure phase is drastically altered as a result of the valence fluctuations and loss of CO, in comparison to the low-pressure monoclinic CO phase (at $T < T_{CCO}$).¹⁶ This is best exemplified by the stark differences in the spectra shown in the insets of Fig. 3. The spectrum recorded at ambient pressure and 110 K ($T < T_M$) shows the conspicuous magnetic hyperfine structure from four Fe sites (analyzed in detail in Ref. 16), which is absent at the same temperature at 16 GPa. This implies that a strong interplay prevails between commensurate CO (onset $T_{CCO} \sim 280$ K) and magnetism (onset $T_M \sim 155$ K) at low pressure. Furthermore, the pressure-induced valence-fluctuating state appears to retain some identity of a paramagnetic state (atomic moment features) from the PHS evident at 113 K (Fig. 3 inset).

ME measurements were also performed in other runs to maximum pressures of ~ 24 GPa and ~ 30 GPa at room temperature in separate experiments, primarily to investigate the high-pressure phase beyond 16 GPa. The spectral profile has persistent asymmetric relative intensities even in the sample pressurized to ~ 30 GPa; see Fig. 2(b). The IS for these high-pressure data exhibit the linear decreasing trend of the valence-fluctuating phase that dominated at ~ 16 GPa. Valence fluctuations (on a timescale of 50 ns) persist to this high pressure.

In conclusion, our direct probing of Fe valences in the archetypal ionic CO compound, Fe_2OBO_3 , shows that condensation into distinct Fe^{2+} and Fe^{3+} valences at 300 K is initially stabilized upon pressurization (4–6 GPa), in accord with prior transport studies. However, further pressurization suppresses this CO; this is first strongly manifested at 11 GPa and culminates at 16 GPa in a valence-fluctuating state involving ~ 50 ns electron exchange dynamics. There is a concomitant drastic modification of the original (ferrimagnetic) low-temperature Fe spin order. This establishes the strong linkage between CO and magnetism in Fe_2OBO_3 and $P \sim 16$ GPa as a newly identified electronic phase transition boundary. Our valence probe reveals persistent electron exchange (confinement of the mobile carrier to the $\text{Fe}^{2+} \leftrightarrow \text{Fe}^{3+}$ pair) to much higher pressures of at least 30 GPa at 300 K. As a result of this work, we are able to present a qualitative (T, P) phase diagram, which merits further detailed investigations.

It is known that there is a comparatively large *onsite* Coulomb repulsion U of 4–6 eV,^{27,28} which, in conjunction with the intersite repulsion V , is required to stabilize CO in this compound. Pressurizing to 16 GPa results in

sufficient alteration of relative values of primarily interchain V and onsite U to disrupt the CO that such Coulomb interactions help to stabilize at low pressure. Whereas charge order may be tuned to suppression at relatively modest pressures in such mixed-valence systems, continued confine-

ment of the mobile carriers may prevail to much higher extremes.

Funding for this project has been derived from both the URC-UJ and the NRF (SA), and both the EPSRC and the Royal Society (UK) and is acknowledged with gratitude.

*Author to whom correspondence should be addressed: grhearne@uj.ac.za

¹Y. Tokura, and N. Nagaosa, *Science* **288**, 462 (2000).

²J. Orenstein, and A. J. Millis, *Science* **288**, 468 (2000).

³J. P. Attfield, *Solid State Sci.* **8**, 861 (2006).

⁴J. v. d. Brink and D. I. Khomskii, *J. Phys.: Condens. Matter* **20**, 434217 (2008).

⁵S.-W. Cheong and M. Mostovoy, *Nat. Mater.* **6**, 13 (2007).

⁶S. Ishihara, *J. Phys. Soc. Jpn.* **79**, 011010 (2010).

⁷M. Angst, P. Khalifah, R. P. Hermann, H. J. Xiang, M.-H. Whangbo, V. Varadarajan, J. W. Brill, B. C. Sales, and D. Mandrus, *Phys. Rev. Lett.* **99**, 086403 (2007).

⁸M. Angst, R. P. Hermann, W. Schweika, J.-W. Kim, P. Khalifah, H. J. Xiang, M.-H. Whangbo, D.-H. Kim, B. C. Sales, and D. Mandrus, *Phys. Rev. Lett.* **99**, 256402 (2007).

⁹This is analogous to the case of spin-frustrated systems involving Kagomé lattices or lattices in which there is triangular connectivity of the sites. In the warwickite oxoborate, we may refer to the system as being “valence” (or geometrically) frustrated because of the triangular connectivity of neighboring sites on different chains. The frustration arises because a situation involving same valence ions as nearest neighbors needs to be minimized, but this cannot be strictly adhered to when there is both triangular connectivity among sites on different chains and charge order along the a axis. As a consequence, various configurations of charge order are degenerate in energy.

¹⁰The low-field magnetization shows marked differences in zero-field cooled and field-cooled susceptibility curves at $T < T_M$; see Ref. 11. Furthermore, the oxoborate has a much lower magnetic ordering temperature $T_M \sim 155$ K compared to magnetite $T_M \sim 860$ K, which may, at least partly, be ascribed to frustrated lattice effects.

¹¹B. Rivas-Murias, F. Rivadulla, M. Sánchez-Andújar, A. Castro-Couceiro, M. A. Señaris-Rodríguez, and J. Rivas, *Chem. Mater.* **18**, 4547 (2006).

¹²M. H. Phan, N. A. Frey, H. Srikanth, M. Angst, B. C. Sales, and D. Mandrus, *J. Appl. Phys.* **105**, 07E308 (2009).

¹³J. P. Attfield, A. M. T. Bell, L. M. Rodríguez-Martínez, J. M. Greneche, R. J. Cernik, J. F. Clarke, and D. A. Perkins, *Nature (London)* **396**, 655 (1998).

¹⁴Y. J. Song, H. X. Yang, H. F. Tian, C. Ma, Y. B. Qin, L. J. Zeng, H. L. Shi, J. B. Lu, and J. Q. Li, *Phys. Rev. B* **81**, 020101 (R) (2010).

¹⁵J. P. Attfield, A. M. T. Bell, L. M. Rodríguez-Martínez, J. M. Greneche, R. Retoux, M. Leblanc, R. J. Cernik, J. F. Clarke, and D. A. Perkins, *J. Mater. Chem.* **9**, 205 (1999).

¹⁶A. P. Douvalis, V. Papaefthymiou, A. Moukarika, T. Bakas, and G. Kallias, *J. Phys.: Condens. Matter* **12**, 177 (2000).

¹⁷A. Akrap, M. Angst, P. Khalifah, D. Mandrus, B. C. Sales, and L. Forró, *Phys. Rev. B* **82**, 165106 (2010).

¹⁸S. Takele and G. R. Hearne, *Nucl. Instrum. Methods B* **183**, 413 (2001).

¹⁹The linewidth of the customized Mössbauer “point” source is ~ 0.35 mm/s for the innermost lines of a 25- μ m-thick Fe foil standard. The areal density of the sample loaded in the cavity is ~ 16 mg/cm². Pressure gradients are about 5–10% of the average quoted pressure. All of these effects lead to line broadening and lower the intrinsic resolution of the experiment. Considerable errors can then be incurred in deriving the abundances from fitting strongly overlapping components. This is the case with the Fe³⁺ and “Fe^{2.5+}” subcomponents, and we have preferred to model these as a single broadened doublet. The Fe²⁺ components have well-resolved signatures at ~ 2 mm/s in the spectral envelope, and abundances can be derived more reliably for these subcomponents.

²⁰The hyperfine interaction parameters, including abundances, are derived from fitting the spectral envelope with Lorentzian sub-components. These are reliable if the features are well resolved in the spectrum. The IS is proportional to the s electron density at the Fe nucleus, and it is influenced by d electron shielding. The QS (doublet splitting) is proportional to the deviation from cubic symmetry of both the surrounding electron configuration and nearest-neighbor atoms. Both IS and QS have distinct “fingerprint” values for Fe²⁺ (d^6) and Fe³⁺ (d^5) ions.

²¹R. H. Herber and H. Eckert, *Phys. Rev. B* **31**, 34 (1985).

²²M. Blume, *Phys. Rev.* **174**, 351 (1968).

²³M. Blume and J. A. Tjon, *Phys. Rev.* **165**, 446 (1968).

²⁴H. H. Wickman, M. P. Klein, and D. A. Shirley, *Phys. Rev.* **152** 345 (1966).

²⁵F. v. d. Woude and A. J. Dekker, *Phys. Status Solidi* **9**, 775 (1965).

²⁶Lowering the temperature appreciably from 300 K will plausibly slow down the electron hopping rate. The spectra of Fig. 3 (16 GPa, inset) suggests that this is to the extent of revealing the paramagnetic character (atomic moment features) of the ions. PHS becomes apparent when spin-relaxation (spin-flip) times are on the order of the Larmor precession time τ_L of the ⁵⁷Fe nucleus. This is a measure of the time required by the nucleus for recognizing the direction of the magnetic hyperfine field at the nuclear site as originated by the atomic moment. For example, the Larmor precession time for a magnetic hyperfine field of 330 kOe at the ⁵⁷Fe nucleus is $\tau_L \sim 5$ ns.

²⁷I. Leonov, A. N. Yaresko, V. N. Antonov, J. P. Attfield, and V. I. Anisimov, *Phys. Rev. B* **72**, 014407 (2005).

²⁸Z. Chen, C. Ma, Y. J. Song, H. X. Yang, H. F. Tian, and J. Q. Li, *Phys. Rev. B* **86**, 045111 (2012).